

# Silicon Defect and Nanocrystal Related White and Red Electroluminescence of Si-rich SiO<sub>2</sub> Based Metal-Oxide-Semiconductor Diode

Chi-Kuan Lin, Gong-Ru Lin\*, Chun-Jung Lin, Hao-Chung Kuo and Chia-Yang Chen

Department of Photonics & Institute of Electro-Optical Engineering,  
National Chiao Tung University  
1001, Ta Hsueh Road, Hsinchu, Taiwan 300, R.O.C.

## ABSTRACT

Silicon defect and nanocrystal related white and red electroluminescences (EL) of Si-rich SiO<sub>2</sub> based on metal-oxide-semiconductor (MOS) diode using transparent electrode contact are reported. The 500nm-thick Si-rich SiO<sub>2</sub> film on n-type Si substrate is synthesized using multi-recipe Si-ion-implantation or plasma enhanced chemical vapor deposition (PECVD). After 1100°C annealing for 3 hrs, the PL of Si-ion-implanted sample at 415 nm and 455 nm contributed by the weak-oxygen bond and neutral oxygen vacancy defects is observed. The white-light EL spectrum was observed at reverse bias, which originates from the tunneling and recombination intermediate state of SiO<sub>2</sub>:Si<sup>+</sup> at a threshold current and voltage of 1.56 mA and 9.6 V, respectively. The maximum EL power of 110 nW is obtained at biased voltage of 25 V. The linear relationship between the optical power and injection current with a corresponding slope of 2.16 μW/A is obtained. The 4-nm nanocrystallite silicon (nc-Si) is precipitated in the 240nm-thick PECVD grown silicon-rich SiO<sub>2</sub> film annealed at 1100°C for 30 min with Indium-tin-oxide (ITO) of 0.8 mm in diameter, which contributes PL at 760 nm. The peak wavelength of the EL spectra coincides well with the PL. The threshold current and voltage are 86 V and 1.08 μA, respectively. The power-current (P-I) slope is determined as 697 μW/A. The carrier injection mechanism is dominated by Fowler-Nordheim(F-N) tunneling.

**Keywords:** Si-rich SiO<sub>2</sub>, Electroluminescence, Nanocrystallite silicon, Defects, Metal-oxide-semiconductor diode

## 1. INTRODUCTION

Various technologies have been proposed to fabricate nanocrystallite silicon (nc-Si) in metal-insulator-semiconductor (MIS) structure, such as electron-beam evaporation,<sup>1</sup> RF-magnetron sputtering,<sup>2</sup> Si-ion-implantation<sup>3</sup> and plasma-enhanced chemical vapor deposition (PECVD),<sup>4</sup> etc. Si-ion-implantation technique is the most commonly method to prepare SiO<sub>x</sub> (x from 0 to 2) thin film. Previous study on the broadband photoluminescence (PL) and electroluminescence (EL) in implanted SiO<sub>x</sub> film have shown strong emission from blue to origin-red and near-infrared regions by implant-induced defects and nc-Si, respectively.<sup>5</sup> With Si-implantation, the quantity of excess silicon or/and the defects in SiO<sub>2</sub> matrices can be precisely controlled by implanting dosage. Alternatively, the SiO<sub>x</sub> film can be synthesized by PECVD growth. Iacona *et al.* have reported the optic luminescence properties of the nc-Si which was prepared by PECVD and demonstrated that the nc-Si size can be controlled by varying the stoichiometry or annealing temperature.<sup>6</sup> The dense nc-Si can be produced in SiO<sub>x</sub> film after annealing, and the PL peak can be varied from 700 nm to 900 nm. Franzo *et al.*<sup>7</sup> has reported the EL of the PECVD-produced SiO<sub>x</sub> film. In this work, the comparisons with two samples prepared by multi-recipe Si-ion implantation and PECVD, respectively, are demonstrated. Different current-voltage and EL characteristics between a thermally annealed indium-tin-oxide (ITO)/SiO<sub>2</sub>:Si<sup>+</sup>/p-Si/Al and an Ag/SiO<sub>2</sub>:Si<sup>+</sup>/p-Si/Ag metal-oxide-semiconductor (MOS) diode are studied.

## 2. EXPERIMENTAL SETUP

The 500nm-thick SiO<sub>2</sub> was grown on n-type (100)-oriented Si substrate by PECVD at pressure of 400 mTorr with tetraethoxysilane (TEOS) fluence of 10 sccm and O<sub>2</sub> fluence of 200 sccm under forward power of 150 W. The multi-energy Si-implanting recipes are 5×10<sup>15</sup> ions/cm<sup>2</sup> at 40 keV, 1×10<sup>16</sup> ions/cm<sup>2</sup> at 80 keV, and 2×10<sup>16</sup> ions/cm<sup>2</sup> at 150 keV. The excess Si atom density is calculated by using a Monte-Carlo simulating program "TRIM". In addition, the

\*grlin@faculty.nctu.edu.tw; phone: 886-3-5712121 ext.56376; fax: 886-3-5716631

secondary ion mass spectrometry (SIMS) of excess Si profile in the  $\text{SiO}_2:\text{Si}^+$  sample is also performed, which is in good agreement with TRIM result. The thermal annealing of  $\text{SiO}_2:\text{Si}^+$  was performed at  $1100^\circ\text{C}$  for 3 h in quartz furnace with flowing nitrogen gas to activate the radiative defects in the  $\text{SiO}_2:\text{Si}^+$ . The  $\text{SiO}_2:\text{Si}^+$  sample was coated a 500-nm Al film for contact on the bottom of substrate by the thermal evaporator. Then the wafer was diced to  $1\text{ mm} \times 1\text{ mm}$  each, and evaporated with Ag on the top of  $\text{SiO}_2:\text{Si}^+$  film to finish the metal-oxide-semiconductor light emission diode (MOS-LED) structure. Another sample of the  $\text{SiO}_x$  film was grown on p-type Si(100) substrate by using a PECVD system at pressure of 70 mtorr with  $\text{SiH}_4$  and  $\text{N}_2\text{O}$  under forward power of 60 W. The  $\text{N}_2\text{O}$  fluence was controlled at 120 scm. After deposition, the  $\text{SiO}_x$  films have been annealed at  $1100^\circ\text{C}$  in  $\text{N}_2$  atmosphere for 30 min. The optical properties of these films have also been studied by photoluminescence (PL) in the same way which has described. Finally, on the top of the  $\text{SiO}_x$  films, 200-nm ITO transparent contacts with diameters of 0.8 mm were evaporated; the 500-nm Al films were also coated on the bottom of the substrate. Then the wafers were also diced to  $1\text{ mm} \times 1\text{ mm}$  square. The Room-temperature and continuous-wave (CW) PL measurements were performed using a He-Cd laser with a wavelength and average intensity of 325 nm and  $5\text{ W/cm}^2$ . The PL and EL from 300 to 1100 nm was detected by a CCD (Ocean Optics, USB-2000). The working distance between the focusing lens and the sample was fine-tuned to maximize the PL intensity. The MOS diode was driven by either a programmable electrometer (Keithley, model 6517) with resolution as low as 100 fA or a voltage source meter (Keithely, 236), using micro-probes (Kar Suss, 253). The optical power were measured using an optical multi-meter (ILX, 6810B). An integrated sphere detector (ILX, OMH-6703B) was employed to collect the light emitted from the surface of the  $\text{SiO}_2:\text{Si}^+$  MOS diode.

### 3. RESULT AND DISCUSSION

The PL and EL spectra of 500-nm thick, 3h-annealed  $\text{SiO}_2:\text{Si}^+$  and Ag/ $\text{SiO}_2:\text{Si}^+$ /n-Si/Al MOS diode under the reverse bias of 20 V are shown in the Fig. 1. During Si implantation (or physical bombardment with high-energy ions), oxygen vacancies and oxygen interstitials (the precursors for the weak oxygen bond defects) are created due to the large number of oxygen atoms displaced from the  $\text{SiO}_2$  matrix. The high-temperature annealing activates enormous radiative defects corresponding to PL at 415, 455 and 520 nm in the  $\text{SiO}_2$  film, which include weak oxygen bond, NOV defects and  $\text{E}'_\delta$  defects. To verify the existence of these irradiative defects in  $\text{SiO}_2:\text{Si}^+$ , the  $\text{SiO}_2:\text{Si}^+$  layer on quartz was studied by absorption spectroscopy<sup>8</sup> and EPR measurement which was made to prove the existence of  $\text{E}'_\delta$  defects revealing the complete activation of  $\text{E}'_\delta$  defects in annealed  $\text{SiO}_2:\text{Si}^+$  for 3 h.<sup>9,10</sup> The high-temperature annealing is expected to produce complete recombination of point defects through the diffusion of mobile oxygen in  $\text{SiO}_2$ . After annealing at  $1100^\circ\text{C}$  for 3 h, the luminescence at both 415 and 455 nm is markedly enhanced by the complete activation of irradiative defects, such as weak oxygen bonds, neutral oxygen vacancies (NOV).<sup>8</sup>

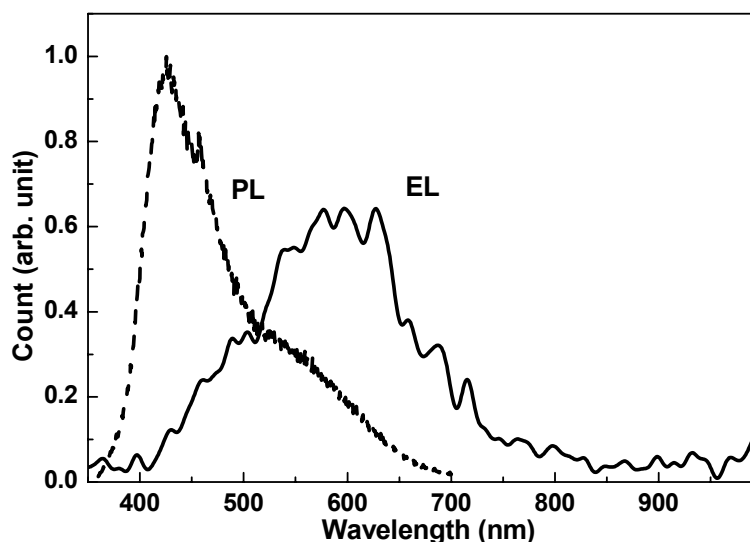


Fig. 1: PL and EL spectra of  $\text{SiO}_2:\text{Si}^+/\text{Si}$  and Ag/ $\text{SiO}_2:\text{Si}^+/\text{n-Si}/\text{Al}$  MOS diode at reverse bias 20 V.

Such a high-temperature annealing condition (1100°C for 3h) has also been employed to precipitate Si nanocrystals. However, the PL spectrum of the annealed SiO<sub>2</sub>:Si<sup>+</sup> samples only show very weak nc-Si dependent fluorescence at the wavelengths range from 700 to 900 nm, which reveal the extremely low density of the nc-Si embedded in the SiO<sub>2</sub>. This result follows from the low-dose implantation process, which yields a low Si excess density of <3% in the SiO<sub>2</sub> matrices. The estimation of 3% excess silicon is calculated by ratio of implanted silicon atoms to silicon atoms in normal SiO<sub>2</sub> matrix. Hence, it is not contradictory that only blue-green emission can be observed from our samples. The EL spectrum of the Ag/SiO<sub>2</sub>:Si<sup>+</sup>/n-Si/Ag MOS diode deviates slightly from that of the PL at threshold voltage about 10 V and more red-shift deviation from PL at 20~30 V. As increasing of voltage as well as electrical field, the luminescence center changes from weak oxygen bond to NOV and finally E'<sub>s</sub> defect owing to hole injection and occupy different valance band of defect. In the proper voltage or electrical field, a very broad band electroluminescence (white electroluminescence, as shown in Fig. 1) can be observed because NOV and E'<sub>s</sub> defects become dominant radiative center concurrently.<sup>8</sup>

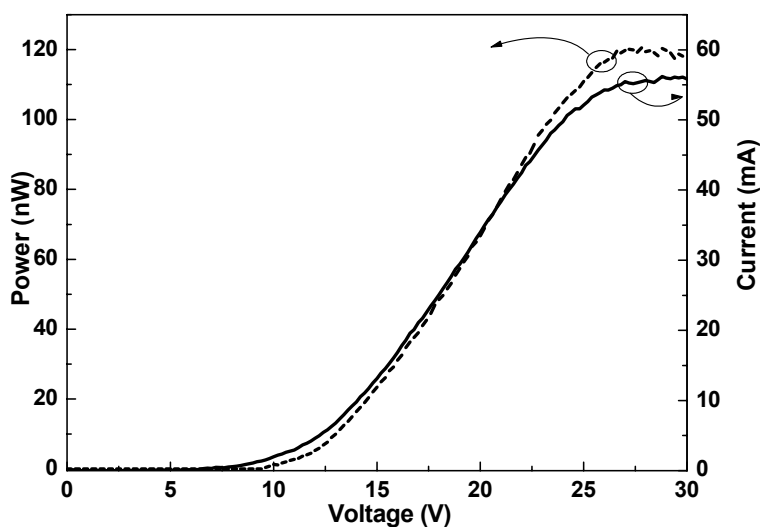


Fig. 2: I-V and P-V response of Ag/SiO<sub>2</sub>:Si<sup>+</sup>/n-Si/Al MOS diode.

The EL spectrum is observed in the MOS diode under reverse bias condition. The Ag film is applied by negative voltage and n-Si substrate with Al contact is applied by positive voltage. The optical power-voltage (P-V) and current-voltage (I-V) curve of the SiO<sub>2</sub>:Si<sup>+</sup> MOS diode driven from 0 to 30 V in magnitude are shown in Fig. 2. The threshold current, voltage and electric field of the MOS diode are 1.56 mA, 9.6 V and 192 kV/cm. The MOS diode can emit maximum power of 110 nW and saturates when pumping voltage is larger than 30 V in magnitude, corresponding to the injected current and electric field 56 mA and 600 kV/cm, respectively. The saturation of injection current is due to the saturation of drift velocity in high electrical field.

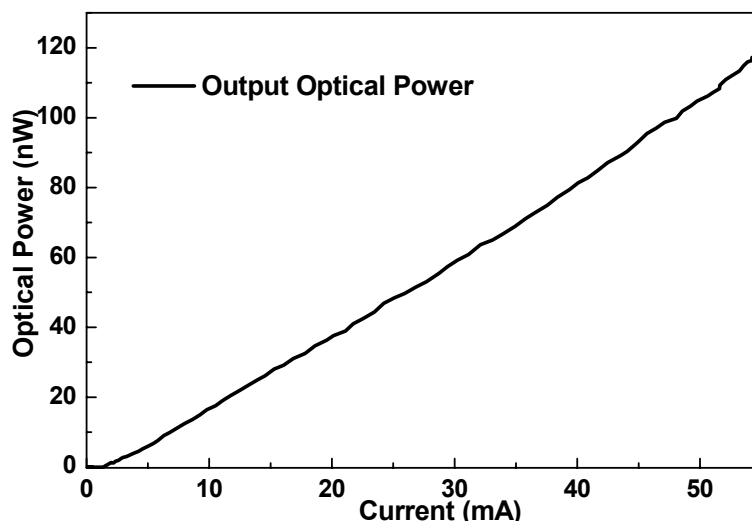


Fig. 3: P-I response of Ag/SiO<sub>2</sub>:Si<sup>+</sup>/n-Si/Al MOS diode.

The linearity diagram between the current and output power was shown in the Fig. 3. The threshold current is 1.5 mA. The optical power could be enhanced by the increasing biased voltage (as well as tunneling current). Consequently, luminescence can be controlled dominantly by carrier injection and ionized the defects in fix rate and electron and hole recombine at high electric field. The power-current (P-I) slope is determined as 2.16  $\mu$ W/A. The EL emits photons via electron-hole recombination processes under a high electric field. Under a reverse bias, an inversion layer can be formed just beneath the SiO<sub>2</sub>/n-Si interface, which accumulates the minority carriers (holes) in n-Si. The transitions of electroluminescence contributed by the weak oxygen bond defects which can emit the deep-blue luminescence and NOV defects at lower biased currents. The white-light EL spectrum of the MOS diode at a bias current of 34 mA is between 400 and 700 nm.

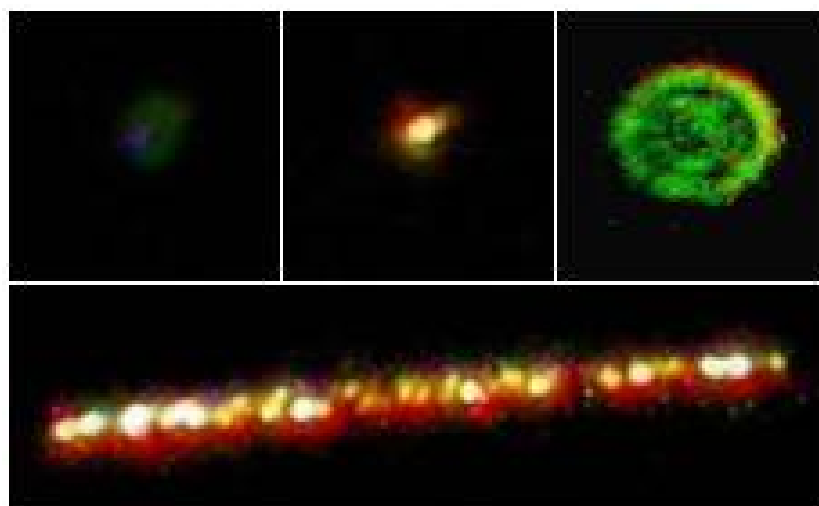


Fig. 4: Upper: The emitting pattern of Ag/SiO<sub>2</sub>:Si<sup>+</sup>/n-Si/Al MOS diode at reverse bias of 10, 20, and 30 V from right to left. Lower: The far-field edge-emitting pattern.

The bright edge-emitting pattern of the Ag/SiO<sub>2</sub>:Si<sup>+</sup>/n-Si/Al MOS diode under reverse bias 20 V (see lower part of Fig. 4). The white-light EL emission is observed at reverse bias of 20 V. The red-shift phenomenon from blue to white and green-yellow light is also observed with the increasing current injection or biased voltage, as shown in the upper part

of Fig. 4. The green EL contributed by  $E'_{\delta}$  defects enhances when the bias current becomes extremely high. With increasing bias, the tunneling electrons and holes can be trapped and subsequently recombine in the occupied states of weak oxygen bond defect, NOV defects, and  $E'_{\delta}$  defects. A higher electric field increases the band bending in the accumulation layer, which facilitates the tunneling of holes from the n-Si substrate to the ground states of NOV and  $E'_{\delta}$  defects. Such an operation greatly enhances the transitions contributing to the blue-yellow luminescence. A stronger bias seriously bends the inversion layer beneath the  $\text{SiO}_2:\text{Si}^+/\text{n-Si}$  interface and thus greatly accumulates the holes at lower states, which subsequently tunnel into the  $E'_{\delta}$  defects at higher energy levels. This effect results in longer luminescent wavelengths at higher bias conditions. Nonetheless, such an impact ionization process usually requires a strong bias, which inevitably causes the substrate to overheat since the cooling of the MOS diode is not efficient. In particular, a forward bias fails to induce EL since the holes can hardly be injected from the positively biased metal contact.

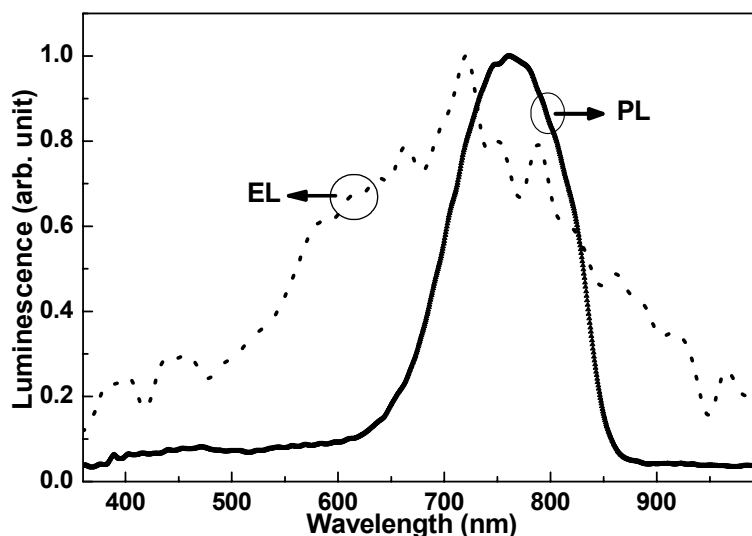


Fig. 5: PL and EL spectra of ITO/SiO<sub>x</sub>/p-Si/Al MOS diode at forward bias voltage 100 V.

The PL and EL spectra of SiO<sub>x</sub> sample produced by PECVD and post-annealing 30 min are shown in the Fig. 5. The PL peak wavelength is about 760 nm and the wavelength range from 650 nm to 850 nm is contributed by dense nc-Si in the SiO<sub>x</sub> matrix. The contribution of weak oxygen bond and NOV defect was not found because the PECVD process introduced less interstitials and vacancies via the structural damage. The emitted wavelength is less small than that from SiO<sub>x</sub> sample which was contained 46 at % of excess Si, annealed at 1100°C for 1h discussed by Iacona *et al.*<sup>6</sup> The reason of such difference can be attributed to the shorter annealing time which can affect the size of nc-Si. Moreover, the shorter annealing time also makes the  $E'_{\delta}$  defects incompletely transfer to nc-Si and the less contribution of  $E'_{\delta}$  defects can be seen around 650 nm to 700 nm in PL spectrum. The EL spectral peak was obtained at the wavelength of 760 nm owing to the recombination of electrons and holes at nc-Si clusters by carrier injected with impact ionization scheme.<sup>7</sup> The EL spectrum was detected under the forward voltage of 100 V and the tunneling current of 9.95  $\mu\text{A}$ . The same wavelength light emission can be also discovered under reverse bias but less intense. Such EL occurs via the tunneling current, and the combination scheme is distinguished from defect-induced sample. The difference of the combination is that the electrons impact the nc-Si and produce electrons and holes in one nc-Si, and two carriers due to the confinement of SiO<sub>2</sub> recombine in nc-Si cluster without accelerating under the high electric field. We also observed that the EL spectrum range from 550 to 850 nm is much broader than PL. The reason of broad wavelength may result from the 700 to 850 nm range luminescence attributed by nc-Si and the defect in oxide contributed the luminescence range of 550 to 700 nm at the center wavelength of 660 nm which is also discovered by Franzo *et al.*<sup>7</sup> but more weak and narrow. The shorter annealing time makes the incomplete transformation of  $E'_{\delta}$  defects and contributes the strong EL between 500 nm to 750 nm range compatible with nc-Si in intensity. Besides, we has also discovered the nc-Si by dark

the bright TEM picture and the calculated size of nc-Si of 4-5 nm coincides with the luminescence wavelength of 750 nm.

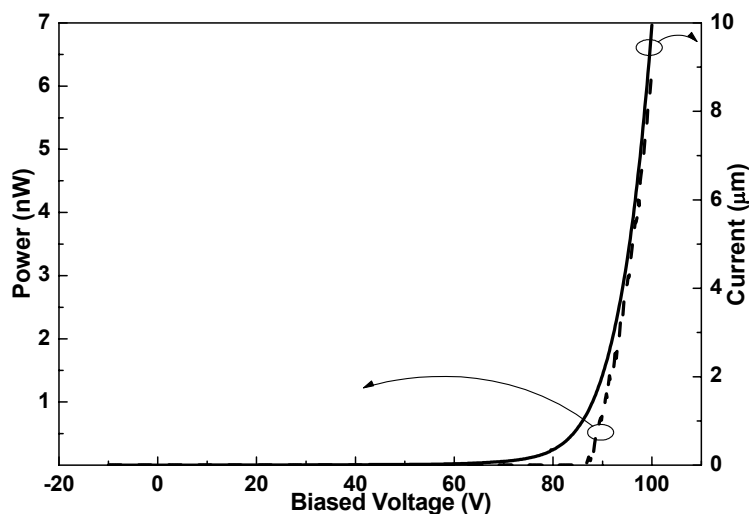


Fig. 6: I-V and P-V response of the ITO/silicon-rich SiO<sub>2</sub>/p-Si/Al MOS diode.

The I-V and P-V curve have also been shown in Fig. 6. The threshold voltage is 86 V, corresponding to the electric field of 3.58 MV/cm and threshold current of 1.08 µA. The carrier injection mechanism is due to tunneling scheme because of its exponentially increasing with voltage linearly increasing

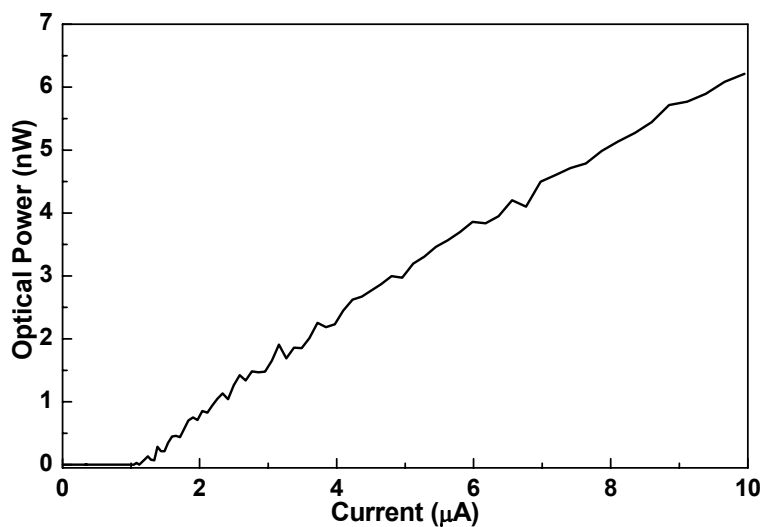


Fig. 7: P-I response of the ITO/silicon-rich SiO<sub>2</sub>/p-Si/Al MOS diode.

Above the threshold, the output optical power and injection current can be a linear relation as shown in Fig. 7. The power-current (P-I) slope is determined as 697 µW/A which is much larger than that in implant sample.

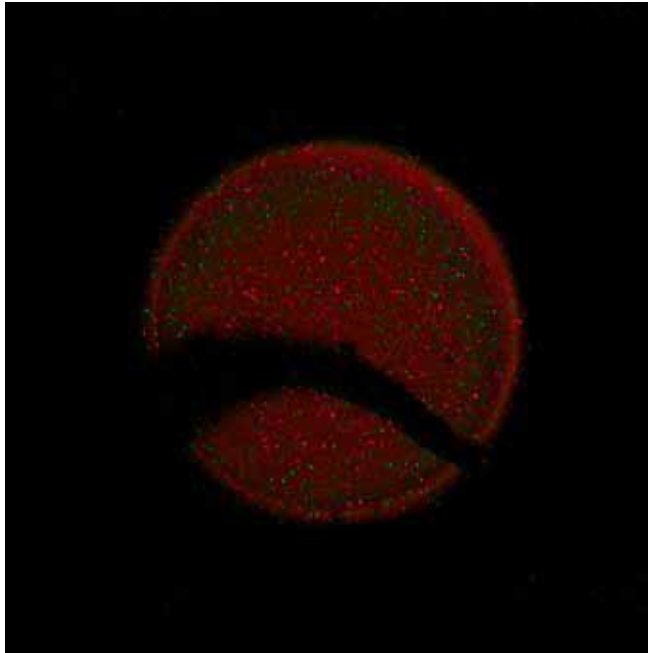


Fig. 8: The emitting pattern of ITO/silicon-rich SiO<sub>2</sub>/p-Si/Al MOS diode

In comparison with the defected-related emitting pattern, a near-infrared surface emission for the ITO/silicon-rich SiO<sub>2</sub>/p-Si/Al MOS diode at forward bias 100 V is shown in Fig. 8. The I-V curve of MOS diode of PECVD grown SiO<sub>x</sub> exhibits higher threshold voltage but lower current than that on Si-implanted SiO<sub>x</sub>. The reason is due to that the PECVD process could grown less non-radiated and irradiated defect in SiO<sub>x</sub> film and after shortly 30-min annealing at 1100 °C, the oxide structure surrounds the nc-Si more pure which makes the current hard to tunneling. In contrary, the ion-implantation introduces more dangling bond defects than PECVD for synthesizing the Si-rich SiO<sub>2</sub> and even during the long time annealing (3h), the defect effect has been activated completely including the non-radiated defect. These activated non-radiated defects raise the current tunneling route and that is why the efficiency of ion-implanted sample is greatly lower than PECVD sample.

#### 4. CONCLUSION

By using multi-recipe Si implantation and PECVD deposition, the Si defect and nanocrystal related white-light and near-infrared electroluminescences of PECVD-grown and Si-implanted Si-rich SiO<sub>x</sub> are studied using an ITO/SiO<sub>x</sub>/p-Si/Al and an Ag/SiO<sub>x</sub>:Si<sup>+</sup>/p-Si/Ag metal-oxide-semiconductor diodes, respectively. The 500nm-thick Si-rich SiO<sub>x</sub> film on n-type Si substrate is synthesized using multi recipe Si-implantation or plasma enhanced chemical vapor deposition (PECVD). After 1100°C annealing for 3h, the PL of Si-ion-implanted sample at 415 nm and 455 nm contributed by the weak-oxygen bond and neutral oxygen vacancy defects is observed. The white-light EL spectrum was observed at reverse bias, which originates from the tunneling and recombination intermediate state of SiO<sub>2</sub>:Si<sup>+</sup> at a threshold current and voltage of 1.56 mA and 9.6 V, respectively. The maximum EL power of 110 nW is obtained at biased voltage of 25 V. The linear relationship between the optical power and injection current with a corresponding slope of 2.16 μW/A is obtained. The 4-nm nanocrystallite silicon (nc-Si) is precipitated in the 240nm-thick PECVD grown silicon-rich SiO<sub>x</sub> film annealed at 1100°C for 30 min with Indium-tin-oxide (ITO) of 0.8 mm in diameter, which contributes PL at 760 nm. The peak wavelength of the EL spectra coincides well with the PL. The threshold current and voltage are 86 V and 1.08 μA, respectively. The power-current (P-I) slope is determined as 697 μW/A. is much larger than that in implant sample.

#### ACKNOWLEDGEMENT

This work was supported in part by National Science Council under grant NSC93-2215-E-009-007.

## REFERENCE

1. Q. Ye, R. Tsu, and E. H. Nicollian, *Phys. Rev. B* **44**, 1806 (1991).
2. K. Toshiakiyo, M. Fujii, S. Hayashi, *physica E*, **17**, 451 (2003).
3. A. Pèrez-Rodríguez, O. González-Varona, B. Garrido, P. Pellegrino, J. R. Morante, C. Bonafos, M. Carrada, and A. Claverie, *J. Appl. Phys.* **94**, 254 (2003).
4. D. Pacifici, E. C. Moreira, G. Franzo, V. Martorino, and F. Priolo, *Phys. Rev. B* **65**, 1441091-1 (2002).
5. T. Matsuda, K. Nishihara, M. Kawabe, H. Iwata, S. Iwatsubo, and T. Ohzone, *Solid State Electro.*, **48**, 1933 (2004).
6. F. Iacona, F. Frazo, E. C. Moreira, D. Pacifici, A. Irrera, and F. Priolo, *Materials Science and Engineering C* **19**, 377 (2002).
7. G. Franzo, A. Irrera, E.C. Moreira, M. Miritello, F. Iacona, D. Sanfilippo, G. Di Stefano, P. G. Fallica, and F. Priolo, *Appl. Phys. A* **74**, 1 (2002).
8. Gong-Ru Lin and Chun-Jung Lin, *J. Appl. Phys.* **95**, 8484 (2004).
9. K. Vanheusden and A. Stesmans, *J. Appl. Phys.* **74**, 275 (1993).
10. Y. Sakurai and K. Nagasawa, *J. Appl. Phys.* **86**, 1377 (1999).